ANALYSIS OF GAS ABSORPTION TO A THIN LIQUID FILM IN THE PRESENCE OF A ZERO-ORDER CHEMICAL REACTION

S. Rajagopalan and M.M. Rahman
Department of Mechanical Engineering
University of South Florida
Tampa, Florida

SUMMARY

The paper presents a detailed theoretical analysis of the process of gas absorption to a thin liquid film adjacent to a horizontal rotating disk. The film is formed by the impingement of a controlled liquid jet at the center of the disk and subsequent radial spreading of liquid along the disk. The chemical reaction between the gas and the liquid film can be expressed as a zero-order homogeneous reaction. The process was modeled by establishing equations for the conservation of mass, momentum, and species concentration and solving them analytically. A scaling analysis was used to determine dominant transport processes. Appropriate boundary conditions were used to solve these equations to develop expressions for the local concentration of gas across the thickness of the film and distributions of film height, bulk concentration, and Sherwood number along the radius of the disk. The partial differential equation for species concentration was solved using the separation of variables technique along with the Duhamel's theorem and the final analytical solution was expressed using confluent hypergeometric functions. Tables for eigenvalues and eigenfunctions are presented for a number of reaction rate constants. A parametric study was performed using Reynolds number, Ekman number, and dimensionless reaction rate as parameters.

At all radial locations, Sherwood number increased with Reynolds number (flow rate) as well as Ekman number (rate of rotation). The enhancement of mass transfer due to chemical reaction was found to be small when compared to the case of no reaction (pure absorption), but the enhancement factor was very significant when compared to pure absorption in a stagnant liquid film. The zero-order reaction processes considered in the present investigation included the absorption of oxygen in aqueous alkaline solutions of sodiumdithionite and rhodium complex catalyzed carbonylation of methanol. Present analytical results were compared to previous theoretical results for limiting conditions, and were found to have very good agreement.

INTRODUCTION

Mass transfer with chemical reactions into thin films has been the subject of many theoretical and experimental investigations. Understanding the process of gas absorption into thin films and its effect on the chemical kinetics of the associated reactions is very important in chemical process industries. Absorption of oxygen into thin films is important in medical engineering. Wetted wall columns are being extensively used in mass transfer studies. The present study presents a detailed theoretical analysis of gas absorption to a thin liquid film adjacent to a horizontal rotating disk. This kind of absorption process is useful in a microgravity environment where usual falling film columns cannot be established and the rate of transport can be enhanced by the introduction of fluid acceleration by an alternative approach such as rotation. In addition to its fundamental scientific contribution and possible application in space based chemical processes, the results of this research will be useful for the design of a spacecraft thermal management system using absorption heat pump.

In the past, there has been a number of studies on mass transfer to a falling liquid film. Olbrich and Wild [ref. 1] studied the diffusion from the free surface into a liquid film in laminar flow over a sphere, a cone and a cycloid of revolution. They used the Laplace transform technique to solve the governing differential equations followed by the application of the residue theorem. Gas absorption with zero-order reaction for a liquid moving in a plug flow was studied by Astarita and Marrucci [ref. 2] Riazi and Faghri [ref. 3] analyzed the gas absorption in a laminar falling film with zero-order reactions. The differential equations were solved by the method of separation of variables, and the subsequent solution was given using an infinite series of hypergeometric functions. They also presented the enhancement factor when compared to the absorption rates in a stagnant liquid film found from a simple penetration model. A simplified form of the enhancement factor was derived for specific conditions.

The overall reaction rate in a gas-liquid reaction is controlled by the physical mass transfer rate and/or by the chemical reaction rate. Two models are generally used to describe the transfer mechanism, viz., the film model and the penetration model. The film model postulates a stagnant film at the surface of the liquid next to the gas . While the rest of the liquid is kept uniform in composition, the gas diffuses into the film by molecular diffusion alone. The penetration theory assumes that after some time the interface is renewed by fresh liquid and fresh gas. The elements of gas and liquid leaving the interface are more or less saturated with the absorbed component. Of the two theories, the film model is the simplest and is applied most frequently. Landau [ref. 4] studied the simultaneous interphase mass transfer and a zero-order reaction using the film model. He gave analytical solutions for three regimes of the absorption process, viz., low rates of absorption when the reaction goes to completion in the film, higher rates of absorption when it goes to completion in the bulk and, at still higher rates of absorption when it does not go to completion. Van de Vusse [ref. 5] derived expressions for the overall reaction rate for mass transfer with chemical reactions. He used both the film theory and the penetration theory. He showed that at high transfer rates the overall reaction rate approaches the chemical reaction rate. The effect of chemical reaction on the bulk-phase concentration was studied by Nagy and Ujhidy [ref. 6]. They gave a mathematical model to calculate the bulk-phase concentrations in the entire finite reaction rate regime in case of both irreversible and reversible reactions. Analyses of mass transfer in hemodialysers for laminar blood flow and homogeneous dialysate was done by Cooney, Kim and Davis [ref. 7]. The solutions were obtained in terms of confluent hypergeometric functions. They also discussed the application of their mathematical model to systems used in clinical practice.

Mass transfer to a thin film adjacent to a rotating disk surface was studied by Rahman and Faghri [ref. 8]. They gave analytical and numerical solutions to the problem. The analytical solution was obtained using the method of separation of variables and hypergeometric functions. Sherwood numbers and bulk concentration were calculated for different values of Reynolds and Ekman numbers and then the results were compared with that of the numerical finite difference solution. They found that significant enhancement of absorption rate can be obtained when the angular velocity of the rotating disk is increased. Their problem involved pure absorption with no chemical reaction.

Several experimental investigations have also been done to study effect of chemical reactions on mass transfer into a thin liquid film. Jhaveri and Sharma [ref. 9] studied the absorption of oxygen in aqueous alkaline solution of sodium diothionite. The reaction was found to be first order with respect to diothionite concentration below 0.08 g mol/l. and second order with respect to diothionite concentration above 0.08 g mol/l. The reaction was found to be zero order with respect to oxygen for all other diothionite concentrations. Roberts and Danckwerts [ref. 10] studied the kinetics of carbon dioxide absorption in alkaline solutions. They devised a method to eliminate the "stagnant film" end effect on wetted-wall columns. The catalytic effect of arsenite ions on the reaction between carbon dioxide and water was measured. Autocatalytic oxidation of Cyclohexane was investigated by Suresh et al [ref. 11]. The behavior of the reaction was found to be complex arising from the fact that the reaction was autocatalytic and the reaction was zero order in oxygen over the entire absorption range. Astarita [ref. 12]

studied the absorption of carbon dioxide into hydroxide solutions and in carbonate- bicarbonate buffer solutions. The absorption rates were measured for a packed tower column. The kinetics of the absorption of Carbon dioxide in monoethanolamine solutions at short contact times was studied by Clarke [ref. 13]. The rates of absorption of carbon dioxide at contact times of 3 and 20 ms and at gas pressures of 1 and 0.1 atm. was measured. He observed that the heat of reaction influences the rate of absorption. The effect of interfacial turbulence during the absorption of carbon dioxide into monoethanolamine was studied by Brian et al [ref. 14]. They discussed the discrepancies between the theoretical considerations and the available experimental data. They stated that this could be due to the interfacial turbulence driven by surface tension gradients. They found that the use of actual physical mass transfer coefficient during the reaction improves the agreement between the penetration theory model and experimental data. Hjortkjaer and Jension [ref. 15] investigated the kinetics of the Rhodium complex catalyzed carbonylation of methanol. The reaction was investigated at carbon mono-oxide pressures between 1 and 50 atm and in the temperature range of 150 - 225 °C. The reaction was discerned to be zero-order with respect to the reactants, and first order with respect to the catalyst and promoter. The activation energy was found to be 14.7 kcal/gmol.

Although a significant number of research has been done on mass transfer into thin liquid films with simultaneous chemical reactions, especially with respect to falling liquid films, very few work has been done on mass transfer into thin liquid films adjacent to a rotating disk. The present study gives a detailed theoretical analysis of gas absorption into a thin liquid film over a rotating disk in the presence of a zero-order chemical reaction. A theoretical model is developed and the effects of Reynolds number, Ekman number and dimensionless reaction rate are studied.

MATHEMATICAL MODEL

The flow of a thin film adjacent to a horizontal rotating disk is considered in the present study. The system is schematically shown in Figure 1. The film is formed by the impingement of a controlled liquid jet at the center of the disk. The disk rotates about its axis with a constant angular velocity ω. The liquid film enters the gas medium at a radial location $r = r_{in}$. A coordinate system attached to the free surface (Figure 1) is used for the analysis. The following assumptions are made to simplify the problem.

(1) $v \ll u$ or w and $\partial/\partial y \gg \partial/\partial r$. These assumptions are valid since the thickness of the film is much smaller than the radius of the disk.

(2) For a very thin liquid layer there is no significant hydrostatic pressure variation. The pressure everywhere in the film is equal to the ambient pressure.

(3) The gravitational body force is negligible when compared to the centrifugal force even for a moderate rate of rotation.

(4) $w \ll u$ and $u = \omega r$. These assumptions are valid only at a large rate of rotation, and become more appropriate at a larger radii.

Under these assumptions, the average velocity at any radial location can be calculated in a closed form and is given by

$$W = \frac{\omega^2 r \delta^2}{3v} \tag{1}$$

The conservation of mass at any radial location gives

$$Q = 2\pi r W \delta \qquad (2)$$

From equation (1) and (2), the film thickness can be expressed as

$$\delta = \left(\frac{3\nu Q}{2\pi\omega^2 r^2}\right)^{1/3} \qquad (3)$$

The above assumptions simplify the differential equation describing the conservation of gas concentration in the liquid stream. In the presence of a simultaneous zero-order chemical reaction occurring in the liquid phase, this equation is described by

$$v_r \frac{\partial C}{\partial r} = D \frac{\partial^2 C}{\partial z^2} - k \qquad (4)$$

The appropriate boundary conditions to equation (4) are

$$r = r_{in}: \qquad C = 0 \qquad (5)$$

$$z = 0: \qquad C = C^* \qquad (6)$$

$$z = \delta: \qquad \frac{\partial C}{\partial z} = 0 \qquad (7)$$

Equation (4) can be written in a dimensionless form as follows

$$(1 - Y^2)\frac{\partial\psi}{\partial X} = \frac{\partial^2\psi}{\partial Y^2} - \alpha \qquad (8)$$

where

$$X = B^{1/2}[\xi^{8/3} - 1] \qquad (9)$$

and

$$B = \frac{1}{(192)^{1/3}} Re_{in}^{-4/3} E_{in}^{-2/3} Sc^{-1} \qquad (10)$$

Corresponding boundary conditions are given by

$$X=0 \quad and \quad 0 \leq Y \leq 1: \quad \psi = 0 \qquad (11)$$

$$Y=0 \quad and \quad X>0: \quad \psi = 1 \qquad (12)$$

$$Y=Y^* \quad and \quad X>0: \quad \frac{\partial \psi}{\partial Y} = 0 \qquad (13)$$

where

$$Y^* = 1 \qquad when \quad \alpha \leq 2$$
$$= \sqrt{\frac{2}{\alpha}} \qquad when \quad \alpha \geq 2 \qquad (14)$$

In equation (14), $\alpha \leq 2$ corresponds to the case when the maximum depth of penetration is equal to the film thickness.

$\alpha \geq 2$ corresponds to the case when the maximum depth of penetration is less then the film thickness. In that situation, the boundary condition given by equation(13) should be changed to

$$Y=Y^* \quad and \quad X>0: \quad and \quad \frac{\partial \psi}{\partial Y} = 0 \qquad (15)$$

Now α can also be written as,

$$\alpha = \frac{p}{\sqrt{X+B}} \qquad (16)$$

where

$$p = \alpha_{in} \sqrt{B} \qquad (17)$$

Hence, the equation (8) becomes

$$(1-Y^2)\frac{\partial \psi}{\partial X} = \frac{\partial^2 \psi}{\partial Y^2} - \frac{p}{\sqrt{X+B}} \qquad (18)$$

The present system [Equations (18), (11-15)] has non-homogeneity in the differential equation which is a function of the variable X, and in the boundary condition which is a constant. The principle of separation of variables can be used to solve the corresponding problem with the non-homogenity in the differential equation being independent of the variable X. Then Duhamel's theorem [ref. 16] can be applied to obtain the actual solution.

41

Introducing the parameter τ in equation (18), the auxiliary problem can be taken as

$$(1-Y^2)\frac{\partial\phi}{\partial X} = \frac{\partial^2\phi}{\partial Y^2} - \frac{p}{\sqrt{\tau+B}} \qquad (19)$$

and the associated boundary conditions being

$$Y=0 \quad and \quad X>0: \quad \psi=1 \qquad (20)$$

$$X=0 \quad and \quad 0\leq Y\leq 1: \quad \psi=0 \qquad (21)$$

and, if $\alpha\leq2$

$$Y=Y^* \quad and \quad X>0: \quad \frac{\partial\psi}{\partial Y}=0 \qquad (22)$$

or, if $\alpha\geq2$

$$Y=Y^* \quad and \quad X>0: \quad \frac{\partial\psi}{\partial Y}=0 \quad and \quad \psi=0 \qquad (23)$$

Equation (19) along with the boundary conditions (20-23) was solved using the method of separation of variables, thus obtaining the solution to the auxiliary problem as

$$\phi(X,Y,\tau) = \frac{p}{2\sqrt{\tau+B}}Y^2 - \frac{p}{\sqrt{\tau+B}}Y\,Y^* + 1 - \sum_{n=1}^{\infty} C_n\lambda_n^{1/2}Y\exp(-\lambda_n^2 X)$$
$$\times \; \exp(-\lambda_n Y^2/2)M\left(\frac{3-\lambda_n}{4},\frac{5}{2},\lambda_n Y^2\right) \qquad (24)$$

The eigen values, λ_n are given as roots of the following equation.

$$(1-\lambda Y^{*2})M\left(\frac{3-\lambda}{4},\frac{3}{2},\lambda Y^{*2}\right) + Y^{*2}\frac{\lambda(3-\lambda)}{3}M\left(\frac{7-\lambda}{4},\frac{5}{2},\lambda Y^{*2}\right) \qquad (25)$$

The constant, C_n can be determined by using the orthogonal property of the eigen functions, and given as

$$C_n = \frac{\int_0^1 \left(-\frac{p}{2\sqrt{\tau+B}} Y^2 + \frac{p}{\sqrt{\tau+B}} YY^* - 1 \right)(1-Y^2)N_n(Y)dY}{\int_0^1 (1-Y^2)N_n^2(Y)dY}$$ (26)

where, $N_n(y)$ are the eigen functions given by

$$N_n(Y) = \lambda_n^{1/2} Y \exp(-\lambda_n Y^2/2) M \left(\frac{3-\lambda_n}{4}, \frac{3}{2}, \lambda_n Y^2 \right)$$ (27)

and M(a,b,c) is the confluent hypergeometric functions with arguments a,b and c [ref. 17].

The solution to the present auxiliary problem is similar to that obtained by Riazi and Faghri   [ref. 3] for gas absorption in a falling liquid film in the presence of a zero order chemical reaction.

The Duhamel's theorem relates the solution of the auxiliary problem to the original problem and is given by

$$\psi(X,Y) = \frac{\partial}{\partial X} \int_{\tau=0}^{X} \phi(X-\tau,Y,\tau)d\tau$$ (28)

After performing the integration, we get the concentration profile as

$$\psi(X,Y) = \frac{\alpha}{2} Y^2 - \alpha Y^* + 1 - \sum_{n=1}^{\infty} A_n \lambda_n^{1/2} Y \exp(-\lambda_n Y^2/2) \exp(-\lambda_n^2 X)$$
$$\times M \left(\frac{3-\lambda_n}{4}, \frac{3}{2}, \lambda_n Y^2 \right)$$ (29)

where

$$A_n = \frac{\int_0^1 \left(-\frac{\alpha}{2} Y^2 + \alpha YY^* - 1 \right)(1-Y^2)N_n(Y)dY}{\int_0^1 (1-Y^2)N_n^2(Y)dY}$$ (30)

The first fifteen values of λ_n and A_n are listed in Table 1.   The eigen values λ_n were determined from equation (25) by using the bisection method and the corresponding integration constants, A_n were obtained from equation (30). The numerical integration was performed using Simpson' rule. Up to 32 digits were retained for all mathematical calculations though we list only eight digits after the decimal in table 1. This was required to overcome truncation errors during the computation of confluent hypergeometric functions which are periodic in nature.

The Sherwood number for gas absorption can be written as

$$Sh^* = \frac{-\frac{\partial \psi}{\partial Y}\big|_{Y=0}}{1 - \int_0^1 \psi \, dy}$$

(31)

After substituting for ψ from equation (29) into equation (31), the Sherwood number can be written as

$$Sh^* = \frac{\alpha Y^* + \sum_{n=1}^{\infty} A_n \exp(-\lambda_n^2 X) \lambda_n^{1/2}}{-\frac{\alpha}{6} + \frac{\alpha Y^*}{2} + \sum_{n=1}^{\infty} A_n \exp(-\lambda_n^2 X) \lambda_n^{1/2} \int_0^1 \exp(-\lambda_n Y^2/2) Y M \left(\frac{3-\lambda_n}{4}, \frac{3}{2}, \lambda_n\right)}$$

(32)

In order to get a better understanding of the change of absorption rate with the flow rate and the rate of rotation, Sherwood number without the film thickness, Sh was also calculated. The Sherwood number, Sh can be related to Sh^* by the relation

$$Sh = Sh^* \left(\frac{v^2}{3gr_{in}^3}\right)^{1/3} Re_{in}^{1/3} \, E_{in}^{-2/3} \, \xi^{2/3}$$

(33)

The influence of the chemical reaction can be evaluated by comparing the rate of gas absorption, G to the rate of gas absorption, G_{∞}^0 of an infinitely deep stagnant liquid with the same physical properties and with no chemical reaction. The ratio, G/G_{∞}^0 is known as the enhancement factor [ref. 3]. The the Enhancement Factor when compared to the case of physical absorption, E_{∞} can be written as

$$E_{\infty} = \frac{Y^* \alpha X + \sum_{n=1}^{\infty} \frac{A_n}{\lambda_n^{3/4}} (1 - e^{-\lambda_n^2 X})}{\sqrt{\frac{4}{\pi} X}}$$

(34)

The influence in the chemical reaction can also be evaluated by comparing the absorption rate, G with the absorption rate, G_o, of the same flow system but in which the chemical reaction is absent. Thus the Enhancement Factor when compared to the case of no chemical reaction but the same flow system, E_o is given by

$$E_0 = \frac{Y^* \alpha X + \sum_{n=1}^{\infty} \frac{A_n}{\lambda_n^{3/4}}(1 - e^{-\lambda_n^2 X})}{\sum_{n=1}^{\infty} \frac{A_n}{\lambda_n^{3/4}}(1 - e^{-\lambda_n^2 X})} \qquad (35)$$

RESULTS AND DISCUSSION

The mathematical model developed in the previous section was used to calculate the mass transfer rates and enhancement factors for some specific flow rates and rates of rotation. The flow system that was considered in the present investigation is shown in figure 1. The fluid enters the gas medium at a radial location $r=r_{in}$ and is dispersed along the radial direction. The gas is absorbed and reacts with the fluid in zero-order simultaneously and the absorbed gas is transported downstream with the flow. It is assumed that the mass of the gas absorbed is negligible compared to the mass of the liquid. The flow remains laminar throughout the physical domain considered in the present investigation. The important dimensionless parameters are: the radial location X, the normal coordinate Y, the concentration Ψ, the Reynolds number Re, the Ekman number E and the reaction parameter α.

The thickness of the liquid film is given by equation (3). As can be seen from the equation, the thickness decreases monotonically with the radius. The thickness depends on the fluid flow rate and the rotational speed. At larger radii, the flow is driven by the centrifugal force. The effects of inertial force are significant only at smaller radii. The present study did not consider the development region near the center of the disk. For a small Ekman number (large rate of rotation), the flow is primarily driven by centrifugal force even at small radial locations. The film height can greatly influence the rate of absorption. Under a very fast reaction, a low diffusion rate, or when the thickness of the film is large, the penetration depth remains smaller than the film thickness($\alpha \geq 2$) at the entire flow domain. Under a slow reaction, a very thin film, or a high diffusion rate, the penetration depth becomes equal to the film thickness ($\alpha \leq 2$) after the film has travelled some distance downstream.

The analytical solutions for dimensionless concentration and Sherwood number (dimensionless mass transfer rate) are given by equation (29) and equation (32), respectively.These equations represent the solution as a series of confluent hypergeometric functions, and are valid for any given reaction rate. The solution for the first fifteen sets of eigenvalues (λ_n) and the coefficients (C_n) are presented in Table 1 for different values of α. The eigen values were obtained as roots of equation (25). The bisection method was used to calculate the eigenvalues. Simpson's rule was used to perform the numerical integration with 5000 intervals. In all numerical computations, 32 digits were retained after the decimal to accurately calculate the values of hypergeometric functions. The values in Table 1 were compared with those presented by Riazi and Faghri [ref. 3] for gas absorption to a falling film with zero order chemical reaction and Olbrich and Wild [ref. 1] and Rahman and Faghri [ref. 10] for the case of $\alpha=0$ (absorption with no chemical reaction). The present results differed slightly from those of Riazi and Faghri [ref. 3]. The difference becomes larger at higher eigen values. It was found that the discrepancy is due to truncation errors in the calculations of Riazi and Faghri [ref. 3] who used double precision arithmetic for their calculations. The results in this paper appears to be more accurate as up to 32 significant digits were used for the calculations and the eigen values and the integration coefficients agree exactly with that of Olbrich and Wild[ref. 1] and Rahman and Faghri[ref. 10] for the limiting case of $\alpha=0$. The eigen values calculated from the equation (25) are independent of α when $\alpha \leq 2$ but it depends on α when $\alpha \geq 2$ (since

$Y^* = \sqrt{(2/\alpha)}$ when $\alpha \geq 2$). It may be noted that for any   given flow rate and speed of rotation, the dimensionless reaction parameter α, varies with the radial location as it is dependent on the local film thickness.

The concentration profile at different radial locations for $\alpha=0.1$ and $\alpha=2$ are shown in figures 2 and 3 respectively. In both these graphs, it can be seen that the concentration increases in the downstream direction at all locations across the thickness of the film. As the liquid film moves downstream, the gas diffuses in and reacts with the film. At values of α less then or equal to 2, the gas can penetrate the entire film thickness. When α is larger then 2, the penetration can extend only through a part of the film thickness. It can be seen in figure 2 that at $\alpha=0.1$, the gas penetrates the entire film thickness when X is larger than 0.05. At larger values of X, the concentration increases all across the film thickness, until at about 0.7, the concentration profile reaches a fully-developed condition. The concentration profile does not change as the film moves further downstream. This profile is shown as $X=\infty$ in the plots. In figure 3, it can be noticed that at $\alpha=2$, the gas penetrates only through the part of the film thickness and part of the liquid remains pure. The penetration depth becomes larger and larger as the film moves downstream, and in the fully developed condition, it just touches the solid wall. The fully-developed concentration profile for different values of α is demonstrated in figure 4. It can be clearly seen from the graph that the reaction goes to completion within a part of the film when $\alpha \geq 2$. As α increases, the fully developed concentration decreases for any particular radial location.

Figures 5 and 6 shows the variation of Sherwood number (Sh and Sh^*) along the radius of the disk for different values of Ekman number. In these plots, both Reynolds number and the chemical reaction rate are preserved constant. In figure 5, it can be noticed that the Sherwood number decreases downstream monotonically. As the Ekman number becomes smaller, the Sh^* also becomes smaller. This is due to the fact that at smaller Ekman number (i.e. at larger rotational speed) the film thickness also becomes smaller. To single out the variation of mass transfer rate with the rotational speed of the disk, Sh is plotted in figure 6. As expected, the Sherwood number increases with a decrease in Ekman number as the actual mass transfer coefficient increases with the increase in rotational speed. The effect of Reynolds number on Sherwood number can be seen in figures 7 and 8. In these plots, the Ekman number and the chemical reaction rate are kept constant. From figure 7 it can be seen that an increase in Reynolds number causes an increase in Sh^*. This is true, since an increase in the flow rate can cause an increase in the mass transfer rate. Figure 8 shows the variation of the Sherwood number (Sh) with the radius at different Reynolds number. It can be noticed that the Sherwood number, Sh decreases monotonically with the radius. For flow over a rotating disk, at smaller radii the flow is dominated by the inertial force and at larger radii, it is dominated by the centrifugal force. Figures 9 and 10 show the variation of the bulk concentration with the radial location, ξ at different values of Ekman and Reynolds numbers. As expected, in both these plots, the bulk concentration increases with the radial location at all values of Reynolds and Ekman numbers.

The effect of reaction rate is shown in figures 11 and 12. The figures show the variation of the Sherwood number and the bulk concentration with the radius for two different chemical reactions. These are the reaction of oxygen with the aqueous alkaline solution of sodium dithionite ($K=6.4 \times 10^2$) and the carbonylation of methanol ($K=1.42 \times 10^6$). Figure 11 shows the variation of Sherwood Number Sh^* along the radius for the two chemical reaction rates considered. The Sherwood number, Sh^* decreases with an increase in rate constant k for both the flow systems considered. When the rate constant is larger, an increase in the mass transfer coefficient might be expected for a given set of fluid properties. But the dimensionless parameter α also depends upon the diffusion rate, D and the solubility of the gas in the liquid, C^*. Thus for a given film thickness, the mass transfer coefficient depends upon the quantity $k/(C^*D)$. Therefore, when two different gas liquid reactions (zero-order) are considered, it would be appropriate to consider the variation of the parameters with respect to the ratio of the quantity k/C^*D. When this quantity is larger, the gas absorption rate increases. This is consistent with the trend seen in

figure 11. The quality k/C^*D for the reaction of sodium dithionite with oxygen is 8.95×10^7 and for the carbonylation reaction it is 5.5×10^7 m^{-2}. Figure 12 shows the variation of bulk concentration with radius for the two different reactions considered in the study. The bulk concentration shows an increase with an increase in the reaction rate.

The enhancement factors (equations 34 and 35) were calculated for different values of X and different combinations of reaction reate, Reynolds number, and Ekman number. It was found that E_∞ is the maximum near the entrance and reduces rapidly with the radius. The larger enhancement near the entrance may be attributed to the smaller concentration boundary layer thickness in that region.

CONCLUSIONS

An analytical solution for the process of gas absorption to a thin film liquid film adjacent to a horizontal rotating disk in the presence of a zero order chemical reaction is presented. The analysis yielded closed form solutions in terms of a series of confluent hypergeometric functions. It was found that the gas can penetrate all across the thickness of the film only if the dimensionless reaction rate α is less than or equal to 2. For $\alpha > 2$, the penetration depth can be only a part of the film thickness. It was also observed that the concentration profile attains a fully developed condition at approximately X=0.7. The rate of mass transfer increased with flow rate as well as with the rate of rotation. The chemical reaction influenced the rate of gas absorption at the free surface. The mass transfer coefficient increased with increase in k/C^*D. The enhancement factor was found to be very significant when compared to absorption in a stagnant liquid film.

NOMENCLATURE

A_n	integration coefficient for n th eigen value (equation 30)
B	constant defined by equation (10)
C	Concentration of dissolved gas in the liquid [kmol m^{-3}]
C^*	Concentration of the dissolved gas at the interface [kmol m^{-3}]
C_n	integration coefficient for n th eigen value (equation 26)
D	liquid phase diffusion coefficient [$m^2 s^{-1}$]
E	Ekman number, $v/\omega r^2$
E_0	enhancement factor for the case of no chemical reaction
E_∞	enhancement factor for the case of infinitely deep stagnant liquid
G	gas absorption rate [kg $m^{-2} s^{-1}$]
G_0	gas absorption rate when the chemical reaction is absent [kg $m^{-2} s^{-1}$]
G_∞^0	gas absorption rate without chemical reaction in an infinitely deep stagnant liquid [kg $m^{-2} s^{-1}$]
k	zero-order reaction rate constant [kmol m^{-3} s^{-1}]
m	dimensionless gas absorption rate
m_0	dimensionless gas absorption rate when the chemical reaction is absent
M	confluent hypergeometric function
p	constant defined by equation (17)
Q	volumetric flow rate [$m^3 s^{-1}$]
r	radial coordinate [m]
Re	Reynolds number, $W\delta/v$
Sc	Schimdt number, v/D
Sh	Sherwood number, $[G(v^2/g)^{1/3}]/\rho D$

Sh*	Sherwood number in terms of the film height, $G\delta/\rho D$
u	velocity in the angular direction [m s^{-1}]
v	velocity in the normal direction [m s^{-1}]
w	velocity in the radial flow direction [m s^{-1}]
W	average velocity along the radius [m s^{-1}]
X	dimensionless coordinate in the radial direction
Y	dimensionless coordinate normal to the plate, z/δ
z	coordinate normal to the plate [m]

Greek symbols

α	dimenesionless reaction parameter, $k\delta^2/C^*D$
δ	film thickness [m]
θ	angular coordinate [rad]
λ	eigen value
ν	kinematic viscosity [m^2 s^{-1}]
ξ	dimesionless radial coordinate, r/r_{in}
ρ	density of the liquid [kg m^{-3}]
τ	parameter introduced in the auxiliary problem
Φ	solution of the auxiliary problem given by equation (24)
ψ	dimensionless concentration, C/C^*
ω	angular velocity [rad s^{-1}]

Subscripts

in	condition at entrance
ave	average value across the film thickness
b	mixed-mean (bulk) condition

REFERENCES

1. Olbrich, W.E.; and Wild, J.D.: Diffusion from the Free Surface into a Liquid Film in Laminar Flow over Defined Shapes. Chem. Engg. Sci., vol. 24, 1969, pp. 25-32.

2. Astarita, G.; and Marrucci, G.: Gas Absorption with Zero-Order Chemical Reaction. I. & EC Fund., vol. 2, no. 1, 1963, pp. 4-7.

3. Riazi, M.; and Faghri, A.: Gas Absorption with First-Order Chemical Reaction. AIChE JL., vol.31, 1985, pp. 1967-1972.

4. Landau, J.: Absorption Accompanied by a Zero-Order Reaction. Canad. Jl. Chem. Engg., vol. 68, 1990, pp. 599-607.

5. Van de Vusse, J.G.: Mass Transfer with Chemical Reaction. Chem. Engg. Sci., vol. 16, 1961, pp. 21-30.

6. Nagy., E.; and Ujhidy A.: Model of the Effect of Chemical Reaction On Bulk Concentrations. AIChE Jl., vol. 35, no. 9, 1989, pp. 1564-1568.

7. Conney, D.O., Kim, S.S.; and Davis, E.J.: Analysis of Mass Transfer in Hemodialysers for Laminar Blood and Homogeneous dialystate. Chem. Engg. Sci., vol. 29, 1974, pp. 1731-1738.

8. Rahman, M.M.; and Faghri, A.: Gas Absorption and Solid Dissolution in a Thin Liquid Film on a Rotating Disk. Int. Jl. Heat and Mass Tran., vol. 36,no. 1, 1993, pp. 189-199.

9. Jhaveri, A.S.; and Sharma, M.M.: Absorption of Aqueous Solutions of Sodium Dithionite. Chem. Engg. Sci., vol. 23, 1968, pp. 1-8.

10. Roberts, D.; and Danckwerts, P.V.: Absorption in alkaline Solutions-I Transient Absorption Rates and Catalysis by Arsenite. Chem. Engg. Sci., vol. 17, 1962, pp. 961-969.

11. Suresh, A.K., Sridhar, T.; and Potter, O.E.: Autocatalytic oxidation of Cyclohexane - Mass Transfer and Chemical Reaction. AIChE Jl., vol. 34, no. 1, 1988, pp. 81-93.

12. Astarita, G.: Absorption of Carbon dioxide into Alkaline Solutions in Packed Towers. I & EC Fund., vol. 3, no. 4, 1963, pp. 294,297.

13. Clarke, J.K.A.: Kinetics of Absorption of Carbon dioxide in Momoethanolamine. Solutions at Short Contact Times. I & EC Fund. vol. 3, no. 3, 1964, pp. 239-245.

14. Brian, P.L.T., Vivian, J.E.; and Matiatos, D.C.: Interfacial Turbulence during the Absorption of Carbon Dioxide into monoethanolamine. AIChE Jl. vol. 13, no. 1, 1967, pp. 28-36.

15. Hjortkjaer, J.; and Erren. W.J.: Rhodium Complex Catalyzed Methanol Carbonylation. Ind. Engg. Chem. Prod. Res. Dev. vol 15, no. 1, 1976, pp. 46-49.

16. Ozisik, M.N.: Heat conduction. Wiley, 1980.

17. Abarmowitz, M.; and Stengun. I.A.: Handbook of Mathematical Functions with Formulas, Graphs and Mathematical Tables. National Bureau of Standards, Department of Commerce, Washington DC, 1972.

TABLE 1. Eigen values and Integration Coefficients

| No | λ_n | C_n | | | $\alpha=3$ | | $\alpha=4$ | |
		$\alpha=0$	$\alpha=0.1$	$\alpha=2$	λ_n	C_n	λ_n	C_n
1	2.26311053	1.79238360	1.72977244	0.54016045	2.38906211	0.41660402	2.59139039	0.36164776
2	6.29768520	1.02469014	1.02672555	1.06539830	6.74541597	0.93826498	7.42019229	0.87219849
3	10.30772681	0.79631238	0.79386970	0.74745885	11.11656887	0.72127416	12.28077919	0.72237188
4	14.31279359	0.67455957	0.67511830	0.68573409	15.49931414	0.63800582	17.15401771	0.64786122
5	18.31592741	0.59583217	0.59511046	0.58139800	19.88870854	0.57066555	22.03297228	0.51668786
6	22.31808871	0.53954469	0.53980138	0.56467864	24.28213765	0.52485522	26.91492866	0.51736060
7	26.31968463	0.49671455	0.49637764	0.48997642	28.67816743	0.48388371	31.79863869	0.42056847
8	30.32091973	0.46270665	0.46285379	0.46564935	33.07595966	0.45403568	36.68345574	0.44504888
9	34.32190893	0.43485365	0.43466002	0.43098101	37.47499588	0.41836349	41.56901374	0.39960741
10	38.32272219	0.41149648	0.41159178	0.41340251	41.87493997	0.40073456	46.45509083	0.35605761
11	42.32340476	0.39154207	0.39141699	0.38903440	46.27556533	0.36863628	51.34154512	0.37809093
12	46.32398727	0.37423651	0.37430322	0.37557063	50.67671399	0.36209288	56.22828181	0.31925983
13	50.32449129	0.35904110	0.35895337	0.35728658	55.07827279	0.33499816	61.11523525	0.34052013
14	54.32493248	0.34555884	0.34560810	0.34654405	59.48015860	0.33538518	66.00235857	0.31814302
15	58.32532250	0.33349027	0.33342546	0.32106149	63.88230912	0.31361091	7088961745	0.28518091

50
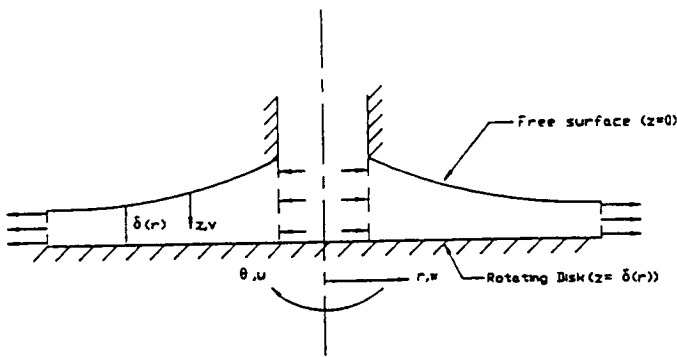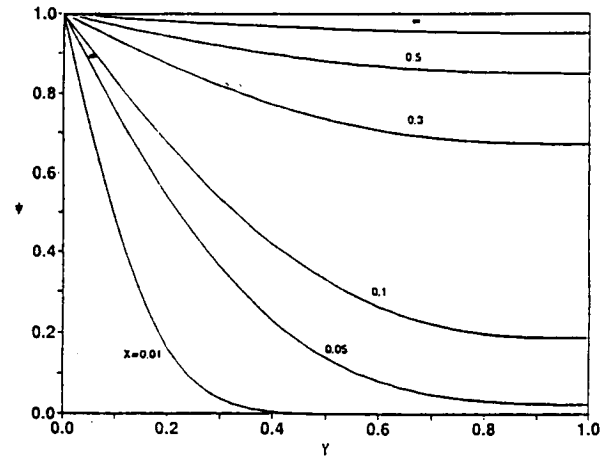
Figure 1 Schematic diagram of the flow system

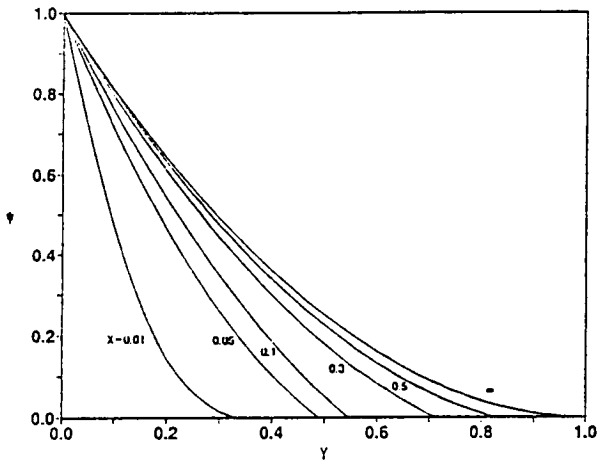Figure 2 Concentration profile for $\alpha=0.1$

Figure 3 Concentration profile for $\alpha=2$

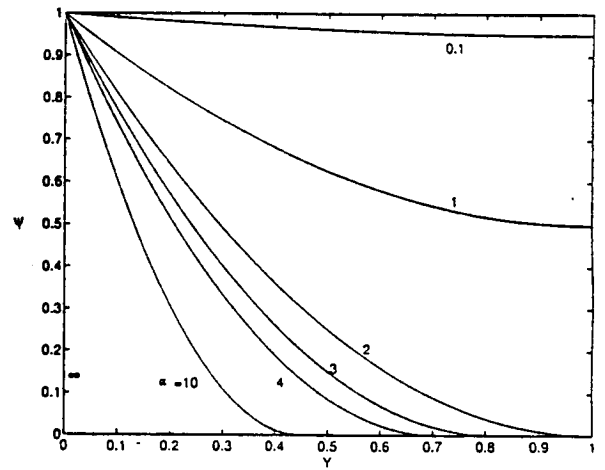
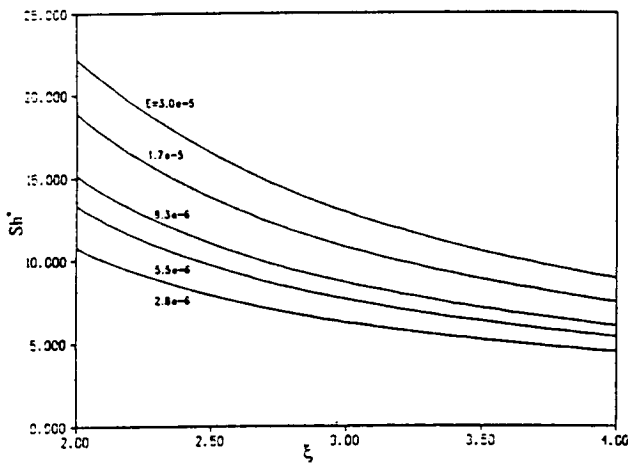Figure 4 Fully-developed concentration distribution at different values of α

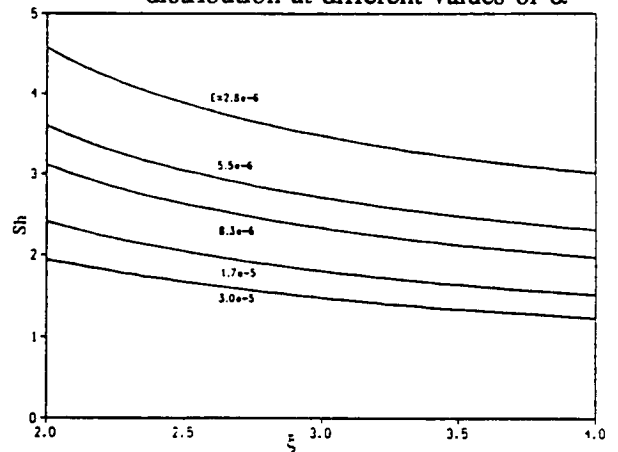Figure 5 Variation of Sherwood number (Sh*) for Re=520 and k=142.5

Figure 6 Variation of Sherwood number (Sh) for Re=520 and k=142.5

51

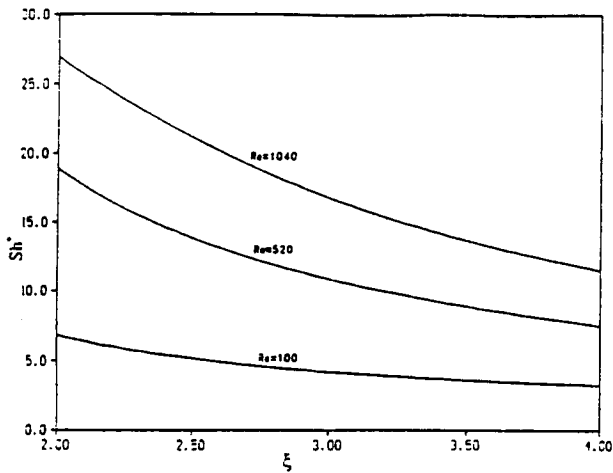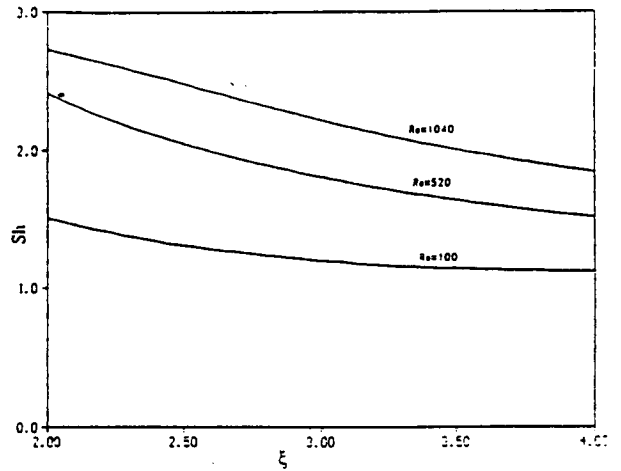Figure 7 Variation of Sherwodd number (Sh*) for $E=1.7\times10^{-5}$ and $k=142.5$

Figure 8 Variation of Sherwood number (Sh) for $E=1.7\times10^{-5}$ and $k=142.5$
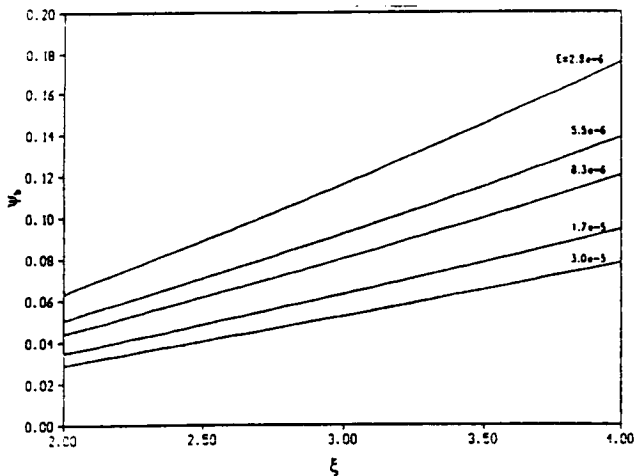
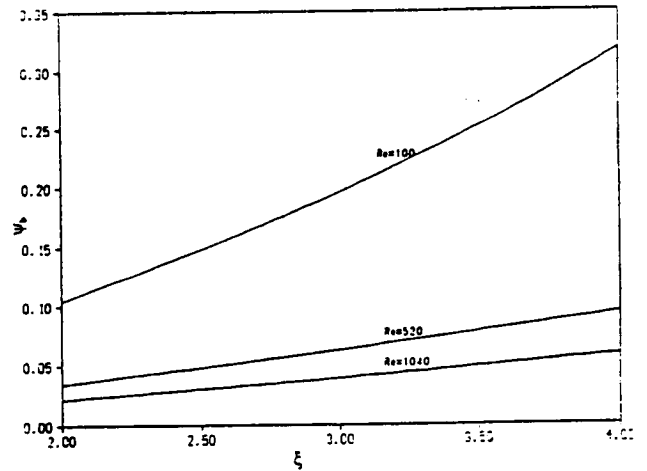Figure 9 Variation of mixed-mean concentration for $Re=520$ and $k=142.5$

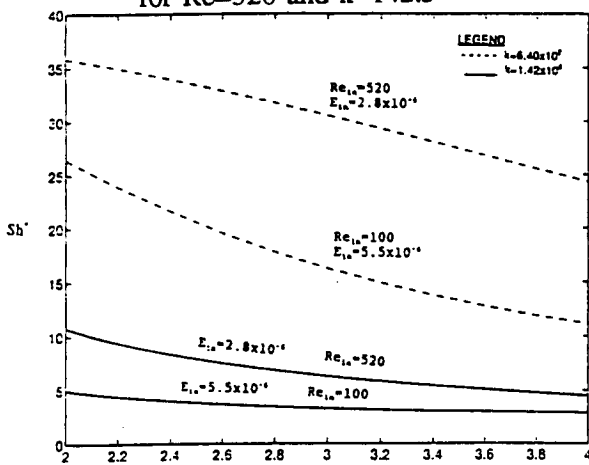Figure 10 Variation mixed-mean concentration for $E=1.7\times10^{-5}$ and $k=142.5$

Figure 11 Comparison of Sherwood number (Sh*) variation for different flow systems
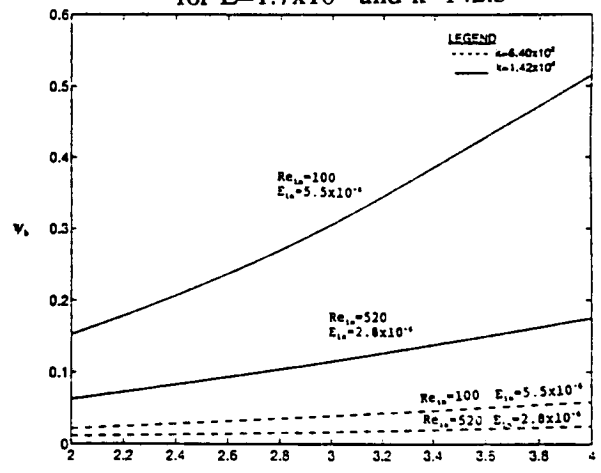

Figure 12 Comparison of mixed-mean concentration for different flow systems